Long-Term Nicotine Abstinence: Craving Regulation and Functional Connectivity Changes in Ex-Smokers

Zanchi, Davide

LONG-TERM NICOTINE ABSTINENCE:

CRAVING REGULATION

AND

FUNCTIONAL CONNECTIVITY CHANGES

IN EX-SMOKERS.

MASTER THESIS IN NEUROSCIENCE

FACULTY OF PSYCHOLOGY

MARCH 18th, 2015

Presented by Davide ZANCHI

Directed by Prof. Dr. med, Sven HALLER

Directed by Prof., Dimitri Van de Ville, P.h.D

Jury member Prof., Francois Lazeyras, P.h.D.

ABSTRACT

Background

Although about one third of smokers tried to quit smoking within the last 12 months, only 3-5% remain abstinent at 6 months. This indicates the presence of long-term modifications in brain networks related to smoking. Using functional magnetic resonance imaging (fMRI), we compared ex-smokers to active and non-smokers to explore these modifications.

Methods

18 non-smokers (29.51 ± 6.70 years, 11 females) 14 smokers (≥10 cigarettes a day > 2 years, 29.31 ± 6.04 years, 10 females) and 14 ex-smokers (>1 year of quitting 30.5 ± 5.70 years, 10 females) were recruited through local and Internet advertising. A block-design fMRI study was performed contrasting smoking cue videos versus control videos. Data analyses include task-related general linear model (GLM), seed based functional connectivity, voxel-based morphometry (VBM) of grey matter and tract based spatial statistics (TBSS) of white matter.

Results

Smoking cue videos versus control videos activated notably the right anterior insula for the contrast ex-smokers versus smokers, an effect correlating with the accumulated dose of nicotine. In addition, ex-smokers, compared to controls and similarly to smokers, showed a persistent decrease in the functional connectivity between anterior insula and anterior cingulate cortex (ACC). The VBM and TBSS analyses excluded potentially confounding grey or white matter alterations.

Conclusion

Long-term nicotine abstinence in ex-smokers yields a dose-related alteration in brain activation of the right anterior insula and furthermore persistent functional connectivity changes including anterior insula and ACC. This indicates persistent brain network changes even more than one year after smoking cessation.

Abbreviations

ACC	anterior cingulate cortex
BET	brain extraction tool
COPE	contrast of parameter estimates
FLAME 1	FMRIB's Local Analysis of Mixed Effects
fMRI	functional magnetic resonance imaging
GM	grey matter
IFG	inferior frontal gyrus
MCFLIRT	intra-modal motion correction tool
OFC	orbito-frontal cortex
PreCG	pre-central gyrus
PostCG	post-central gyrus
raINS	right anterior insula
WM	white matter

Key words: Smokers, Ex-smokers, Long-term Nicotine abstinence, Anterior cingulate cortex, Anterior Insula.

ACKNOLEDGMENTS

At the end of this adventure I want to thank the people that helped me and shared this journey with me:

I want to thank Prof. Van de Ville that accepted me in his lab, supervised me and supported me even beyond what is supposed for a master student. “Give it a try!”

I’m equally grateful to Prof. Haller for his courage and patience with me. One sentence is not enough to thank him. Simply, none of this could have been possible without him.

I want to thank Prof Lazeyras for having welcomed me at the CIBM and made me feel a member of the lab with no differences with the other researchers.

A special thanks to Kirsten Emmert, a great colleague and a real friend!

I thank my family for the support they gave me. Believing in me even when I didn’t.

Finally I want to thank my girlfriend for our journey together, the greatest adventure.

Table of Contents

1. INTRODUCTION

The following study was carried on using functional magnetic resonance imaging (fMRI) that measures the blood oxygen level dependent (BOLD) changes during neural activity. Here briefly its principles and applications.

Oxygen is delivered to neurons by hemoglobin in red blood cells. When neuronal activity increases there is a higher demand of oxygen that leads to an increase in blood flow to regions of increased neural activity. Hemoglobin is diamagnetic when oxygenated and paramagnetic when deoxygenated. This difference in magnetic properties leads to differences in the MR signal of blood, depending on the degree of oxygenation. Since blood oxygenation changes respect to the levels of neural activity these differences can be used to detect brain activity. fMRI can be used to produce activation maps showing which parts of the brain are involved in a particular mental process (Devlin *et al*, 2005). These properties of fMRI and its application to cognitive and clinical neuroscience lead to the development of a branch that nowadays is known as neuroimaging. The goal of cognitive neuroscience is to identify associations between functions and structures in the brain to identify the specific brain areas behind cognitive processes. Our study will use this technique to investigate brain areas related to the cognitive processes behind nicotine addiction.

In Europe, about the 23% of the European population smokes and smoking is considered the largest single cause of preventable death (OECD Health Data 2012). Interestingly, about 31% of this population tried to quit smoking within

the last 12 months (EU anti-tobacco campaign 2013: ex-smokers are Unstoppable) but the relapse rate in the first month of abstinence is about 80%, and only 3 –5% remains abstinent at 6 months (Gualano et al., 2014; Polosa et al., 2011). Many studies tried to investigate the underlying processes of drug addiction and nicotine craving in particular, but the understanding of underlying mechanisms is still very limited.

From a recent review of George Koob (Koob and Volkow, 2010) that describes brain mechanisms involved in drug craving in humans and animals, craving related to nicotine can be associated to craving related to drug addiction, since the brain areas involved are partially overlapping. There are three stages of the addiction cycle.

1.) Binge/intoxication stage

    Reinforcing effects of drugs engage reward neurotransmitters and associative mechanisms in the nucleus accumbens.

2.) Withdrawal state

    The negative emotional state of withdrawal engages the activation of the extended amygdala.

3.) Preoccupation/anticipation of craving

    This stage involves the processing of conditioned reinforcement in the lateral amygdala and the processing of contextual information by the hippocampus.

The executive control function that allows the extinction of caving depends on the prefrontal cortex and includes representation of contingencies, of outcomes, and their value and subjective states associated with drugs.

In particular, focusing on functional MRI studies on humans (George and Koob, 2013), neuroanatomy of drug craving shows that craving-related information is processed by the orbito-frontal cortex (OFC), anterior cingulate cortex (ACC), and nucleus accumbens during drug-related cues (pictures or videos with triggering stimulations). Craving-related information can be modulated by the external or internal context, stress, and affective states through the involvement of the hippocampus, insula and central nucleus of the amygdala (Gardner, 2011). Activation of the dorso-lateral pre-frontal cortex (DLPFC) modulates craving by its connections to other frontal areas as the OFC, ACC, and nucleus accumbens (Garavan *et al*, 2000). The ventromedial prefrontal cortex (vmPFC) is associated with emotional control and the inhibition of actions with poor deleterious consequences (Lee *et al*, 2013).

Focusing specifically on smoking, there are many fMRI studies on smokers and short term-nicotine abstinence (max. 24 hours), (Carroll, Sutherland, Salmeron, Ross, & Stein, 2013; Ding & Lee, 2013; Geier, Sweitzer, Denlinger, Sparacino, & Donny, 2014; Sweitzer et al., 2013), yet very few studies on ex-smokers and long-term nicotine withdrawal (Nestor, McCabe, Jones, Clancy, & Garavan, 2011). Due to this bias towards short-term abstinence studies the brain regions commonly related to nicotine craving are valid in active smokers only (Lerman et al., 2014): the anterior and posterior cingulate cortex (ACC, PCC) as areas responsible for processing of craving-related information, while craving modulation occurs through ventral areas as the insula (Brody et al., 2004; Courtney, Ghahremani, London, & Ray, 2014; Huang et al., 2014).

On the contrary, in the scientific community there is a lack of definitive understanding related to which brain areas underlie long-term nicotine abstinence. To our knowledge only one paper was published on ex-smokers and fMRI to assess the neural substrates that promote nicotine abstinence in a broader timeline (Nestor, McCabe, Jones, Clancy, & Garavan, 2011). The main findings of this study revealed that pre-frontal cortical activity, involving the insula through a top-down control, might be important to promote successful abstinence.

The insula is a key area of the human brain involved in regulation of the body's homeostasis, self-awareness and cognitive functioning. Its role in addiction and in smoking in particular was suggested by Naqvi (Naqvi *et al*, 2007), showing that smokers with brain damage involving the insula were more likely than smokers with brain damage not involving the insula to undergo a disruption of smoking addiction. Theses patients showed an increased ability to quit smoking immediately, without relapse and without persistence of the urge to smoke.

A recent review of Naqvi (Naqvi *et al*, 2014) identifies three main, distinct and opposite functions of the insula: 1) appetitive motivational processes that drive addictive behavior, 2) interoceptive functions that are relevant to drug addiction, and 3) impulse control and decision-making processes that modify addictive behavior according to conflicting goals and negative consequences.

The following study was designed to understand the changes in neural activity that lead to the promotion of long-term nicotine abstinence, trying to identify the main brain areas responsible for craving urge and craving regulation in ex-smokers (>1 year of quitting) compared to non-smokers and smokers during viewing of smoking related videotapes. Later, we investigated if the strength of the activations in the found areas was related to behavioral variables, such as the nicotine dose (pack-years). Finally, we tested how the functional connectivity changes in the three groups, hypothesizing that the ex-smokers occupy an intermediate position between the smokers and non-smokers.

The study presented here tries to contribute to a wider view on craving and nicotine related neural processes, moving from the understanding of the mechanisms underlying the neural activity during short-term nicotine withdrawal to the comprehension of the ones of long-term abstinence.

2. METHODS

2.1. Participants

The local institutional ethical committee approved this study, and all participants gave written informed consent before inclusion. Forty-six subjects (18 non-smokers, 14 smokers, 14 ex-smokers) were recruited through local and Internet advertising. Inclusion criteria for non-smokers were: No tobacco use in their lifetime and no keen to start smoking in the next months. Inclusion criteria for smokers were: smoking 10 or more cigarettes a day over at least 2 years, no intention to quit smoking in the next months and a period of 15 minutes before the study without smoking to control the craving time. Inclusion criteria for ex-smokers were: abstinence of nicotine for a period of more than 12 months prior to the study, previous smoking period of at least 2 years with 10 or more cigarettes a day. The three groups were matched for gender and age, the ex-smokers and the smokers groups matched also for years of smoking and number of cigarettes smoked a day (Table 1). Exclusion criteria for all the participants included a history of drug or alcohol abuse, major medical disorders and use of psychotropics, stimulants or β-blockers on a regular basis. Ex-smokers were additionally considered ineligible if they reported past or current use of products to facilitate nicotine abstinence (e.g., gum, patches, lozenges, nasal spray and inhalators).

DEMOGRAPHIC VARIABLES				
	non-smokers	ex-smokers	smokers	test
Cases	18	14	14	
Females	11	10	10	n/s
Age	29.5 (6.7)	30.5 (5.7)	29.3 (6.0)	n/s
Year of Smoking		8.1 (4.9)	8.6 (4.5)	n/s
Cigarettes per day		13.3 (3.4)	12.7 (3.1)	n/s
Years since quitting		3.7 (3.0)		

Table1. Essential demographic parameters of the included study groups. Values represent mean (standard deviation).

2.2. fMRI brief introduction and acquisition in our study

In our study, images were obtained using a 3T scanner (Trio; Siemens, Erlangen, Germany) with a standard 32 channel head-coil. FMRI imaging of the whole brain was acquired by echo planar imaging using the following parameters: whole brain coverage, 96x96 matrix, TR=2.5s, TE=30ms, 34 slices, 245 repetitions. In addition, a 3D T1-weighted structural scan (256x256 matrix size, 176 sections, 1x1x1 mm^3, TE=2.3ms, TR=2300ms) and diffusion tensor imaging (DTI) scan (30 diffusion directions b=1000 s/mm^2 isotropically distributed on a sphere, 1 reference b=0 s/mm^2 image with no diffusion weighting, 128x64 matrix, 2x2x2mm voxel size, TE=92ms,TR=9000ms, and 1 average) were acquired.

2.3. fMRI Procedure

Participants underwent fMRI in the time between 3 and 6pm to control for potential effects of the time of day. The paradigm consisted of an on-off block-design with two active conditions (smoking cue and control videos) and a rest condition. The active condition used video cues developed by Brody (Brody *et al*, 2007; Culbertson *et al*, 2011). These cues were filmed from the first person point of view and were 45 sec in length. Each smoking video shows a potential craving situation, such as writing a letter and smoking a cigarette or standing outside of a nightclub smoking a cigarette. The control videos were matched for similar content except for the absence of smoking cues. After each video, a visual analog scale was presented for 2.5 seconds and participants rated the degree of craving using an MR-compatible response box. The rating scale included seven steps from no craving to high craving. After the rating, a rest period consisted of the visual presentation of a fixation cross for 10 seconds. Each run included 5 smoking and 5 control videos in a pseudo-randomized fashion and lasted 612 seconds (Supplementary Figure A). Each participant performed two runs. Before fMRI scanning, participants were instructed on the procedure and became familiar with the task by a training run outside of the MRI scanner.

2.4. Statistical Analysis

Statistical analyses were conducted using GraphPad Prism (Version 6, GraphPad Software, San Diego, USA), Matlab (Version 2014a, The MathWorks Inc., Natick, USA) and FSL (Version 5.0.6, FMRIB, Oxford, UK).

2.5. Analysis of Demographic data

After performing the normality test (D'Agostino- Pearson omnibus test) for all the Demographic variables and the Rating Scores, differences between groups were tested as following: the Gender of the subjects was analyzed by the Kruskal-Walls non-parametric test with the multiple comparison correction Dunn's test, the age by an ordinary one-way ANOVA with Tuckey test for multiple comparison correction, the years of smoking by an unpaired parametric t-Test (Wilcoxon matched-pairs signed rank test) and the number of cigarettes a day by Mann-Whitney non-parametric test.

To test the difference in rating scores between smoking and control videos within each group, the Wilcoxon matched-pairs signed rank test was used.

To analyze the difference between the three groups in the rating scores of smoking videos and control videos separately, the Kruskal-Walls non-parametric test with multiple comparison correction Dunn's test was performed.

2.6. Task-related General Linear Model: brief introduction and its application in our study

An fMRI dataset, can be seen as a set of cuboid elements (i.e., voxels) of variable dimension, each of which has an associated time-series of as many time-points as volumes acquired per session. The goal of a statistical analysis is to determine which voxels have a time-course that correlates with some known pattern of stimulation or experimental manipulation. The first step in fMRI data analysis is the pre-processing of the data (Figure 1) that has the

aim of correcting for artifacts introduced at data acquisition. Furthermore, in the GLM analyses, the time-course of each voxel is modeled as a weighted sum of the known predictor variables plus an error term. The aim of the analysis is to estimate if, and how much each predictor contributes to the variability observed in the voxel's time-course (Monti, 2011).

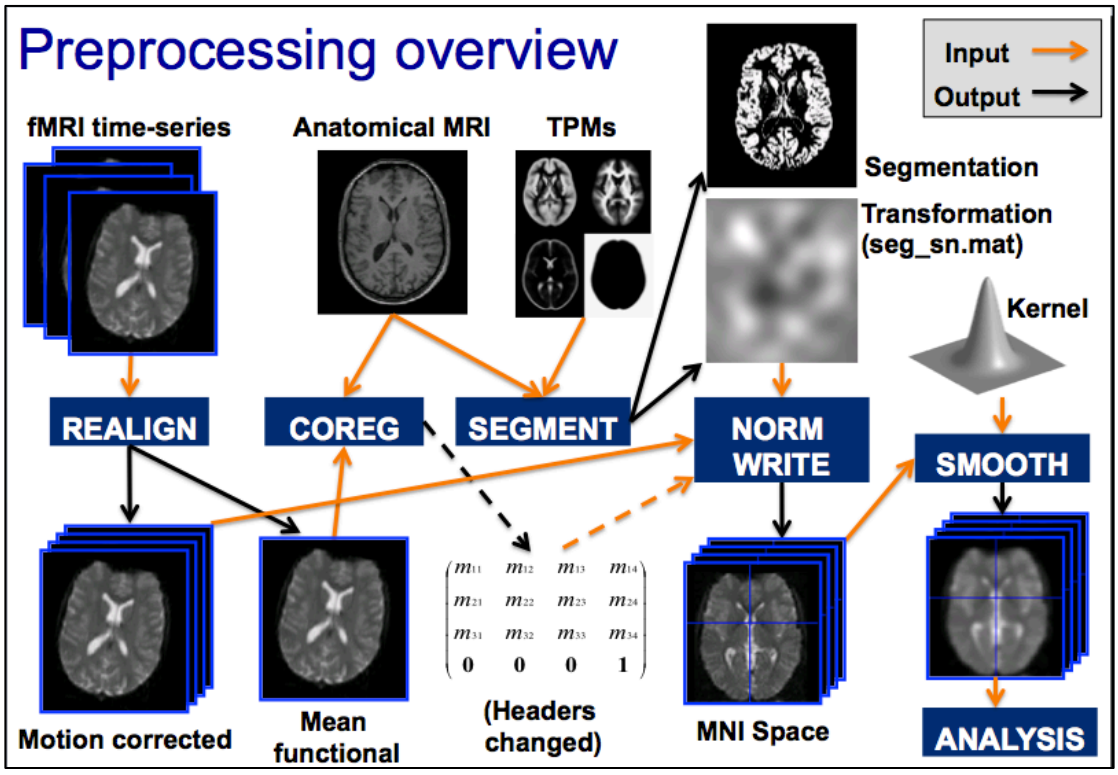

Figure 1: PREPROCESSING OVERVIEW
Functional data are first spatially realigned, motion corrected and co-registered to the anatomical data (successive image volumes in the time series are co-registered to a reference volume. For this purpose a rigid-body transformation is applied with three translational parameters and three rotational parameters). Then the images are normalized and smoothed (5 mm kernel) before group analysis.
Figure available at: http://www.fil.ion.ucl.ac.uk/spm/course/video/#Preproc

In our study, individual pre-processing and individual and group analysis were performed using FSL FEAT (FMRI Expert Analysis Tool).

Preprocessing included brain extraction using FSL's BET (Brain Extraction Tool), motion correction using FSL's MCFLIRT (intra-modal motion correction tool) (Jenkinson *et al*, 2002) and smoothing using FSL's SUSAN (noise reduction uses nonlinear filtering)(Brady, J.M., 1997).

At the first level the contrast smoking videos vs control videos (and vice versa) was calculated separately for each run of each participant using fixed-effects analysis. Next, a second level analysis was conducted for each contrast of each subject that included both runs. Last, a group level analysis between all the 18 non-smokers, 14 smokers and 14 ex-smokers was conducted. In the group level analysis the mixed-effect model (FLAME 1) was used. A permutation-based non-parametric test (randomise, FSL tool) was applied, correcting for multiple comparisons by threshold-free cluster enhancement (Winkler *et al*, 2014). P values <.05 were considered as significant.

2.7. Correlation Between Imaging Data and Pack-Year Smoking History

We tested for possible correlations between regions of the brain that were significantly activated in the contrast of ex-smokers vs. smokers (notably the right anterior insula (raINS)) and the accumulated nicotine dose estimated by pack-year smoking history.

2.8. Seed based Functional Connectivity analysis

Seed regions for functional connectivity analysis were defined from the results of the task-related GLM and previous literature (Nestor, McCabe, Jones, Clancy, & Garavan, 2011). We defined regional masks and extracted region-

averaged time-courses of each subject for the anterior cingulate cortex (ACC), right anterior insula (raINS), and left frontal pole (leftFP). Functional connectivity analysis was performed using a custom-build toolbox in Matlab (Version 2014a, The MathWorks Inc., Natick, USA). In particular, for each subject, we computed all pairwise correlations (3) between the time-courses of these regions to estimate functional connectivity. These values were then submitted, for each connection, first to a one-sample t-test across subjects (to assess significant connectivity) and subsequently to an ANOVA (to assess group differences) with Tukey correction for post-hoc pair-wise comparisons.

2.9. VBM analysis of T1 Images: principles and its application in our study

Voxel based morphometry analyses is a method that uses statistics to identify differences in brain anatomy between groups of subjects. This technique typically uses T1-weighted volumetric MRI scans and basically performs statistical tests across all voxels in the image to identify volume differences between groups. Three are the pre-processing steps that allow the final groups comparisons. First, the MRI scans need to be matched together spatially so that a location in one subject's MRI corresponds to the same location in another subject's MRI. Then Images are segmented into different tissue compartments (gray matter, white matter, and CSF), and analysis is performed separately. Thirdly, the images are smoothed so that the intensity of each voxel is replaced by the weighted average of the surrounding voxels, basically blurring the segmented image. Finally, statistical analysis of the smoothed segmented images are performed with parametric statistics using the general linear model (Whitwell, 2009).

In our study, FSL software packaging was used to perform the VBM analysis. Standard processing steps were used (Smith et al., 2006, 2007). In particular, first BET extraction and tissue-type segmentation were conducted using the corresponding FSL tools (Brain Extraction Tool and FAST4). Subsequently, a non-linear transformation into Montreal Neurological Institute (MNI) reference space was applied and a study-specific Gray Matter (GM) template was created. All the native GM images were then nonlinearly registered to this template. Later on, the images were smoothed with an isotropic Gaussian kernel of 2mm sigma. Finally, by a permutation-based non-parametric test (Randomise, FSL tool) a voxelwise GLM was performed, correcting for multiple comparisons implementing threshold-free cluster enhancement (Smith et al., 2009). Significant results are considered P values >.05. Similar to the GLM analysis, differences in the three groups are tested.

2.10. TBSS analysis of DTI Data: principles and its application in our study

Magnetic resonance diffusion imaging is a technique that provides information about the anatomical connectivity in the brain by measuring the diffusion of water in white matter tracts. Among the different measures, the most commonly derived from diffusion data is the fractional anisotropy (FA), which quantifies local tract directionality and integrity (Smith *et al*, 2007). TBSS, following the same procedure (pre-processing and group analyses) of the VBM, aims to investigate local changes in white matter structure analyzing FA images.

In our study, as the VBM, FSL software packaging was used to analyze DTI data, according to the standard procedure (Smith et al., 2004). First, by a non-linear registration all subjects' fractional anisotropy data was projected onto a mean fractional anisotropy tract skeleton. Later, by using a non-linear registration voxelwise statistical analysis with threshold free cluster enhancement correction for multiple comparisons was performed, with P values <.05 as significant. Differences between all the three groups were tested.

3. RESULTS

3.1. Rating Scores results

Within all of three groups, the smoking videos induce a higher craving rating response than the control videos (P<.01 non-smokers, P<.001 smokers and ex-smokers). Moreover, significant differences are present between the three groups for rating scores of smoking videos (Figure 2). These results confirm that the experimental setup induces more craving during smoking videos than during control videos and that smokers have the highest induced craving perception compared to the other groups, while the ex-smokers can be considered in an intermediate position between smokers and non-smoker. No statistical differences are found in rating scores only for Control videos between the three groups.

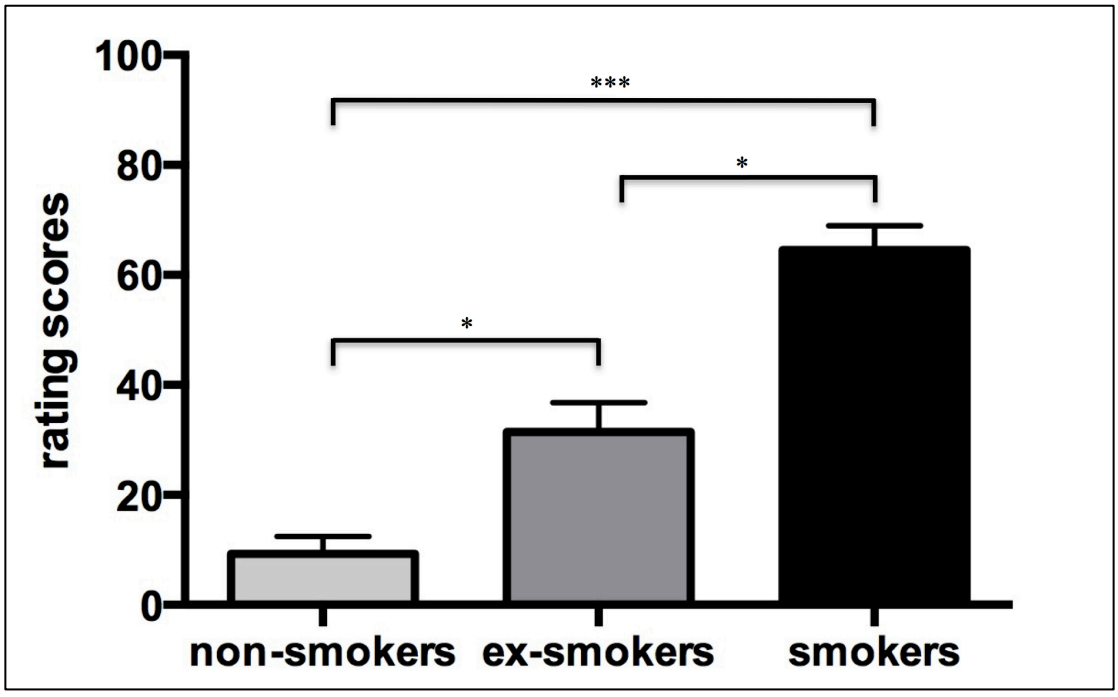

Figure 2: RATING SCORES FOR SMOKING VIDEOS
The rating scores for craving during smoking cue videos (0 = no craving, 100 = maximum craving). Active smokers had significantly higher craving than ex-

smokers ($p<0.05$) and non-smokers ($p<0.001$). ex-smokers had higher craving than non-smokers ($p<0.05$).
The barplots indicate mean values and standard error. * $p<.05$, *** $p<.001$.

3.2. Task-related General Linear Model

In the task-related GLM we considered the contrast of smoking videos versus control videos. The comparison ex-smokers versus smokers revealed significantly greater activations in ex-smokers in the right anterior insula (raINS), right frontal operculum (rFOP), and right inferior frontal gyrus IFG (Figure 3A, Supplementary Table A).

The comparison ex-smokers versus non-smokers revealed a significantly greater activation in ex-smokers bilaterally in the frontal pole (FP), inferior frontal gyrus (IFG), and bilateral anterior insula (aINS) with a higher activation in the right anterior insula (raINS) (Figure 3B).

The comparison ‘smokers versus non-smokers’ revealed increased activation in the anterior cingulate cortex (ACC) and in the cerebellum (Figure 3C). There were no de-activations in the above-mentioned contrasts (see Supplementary Figure B).

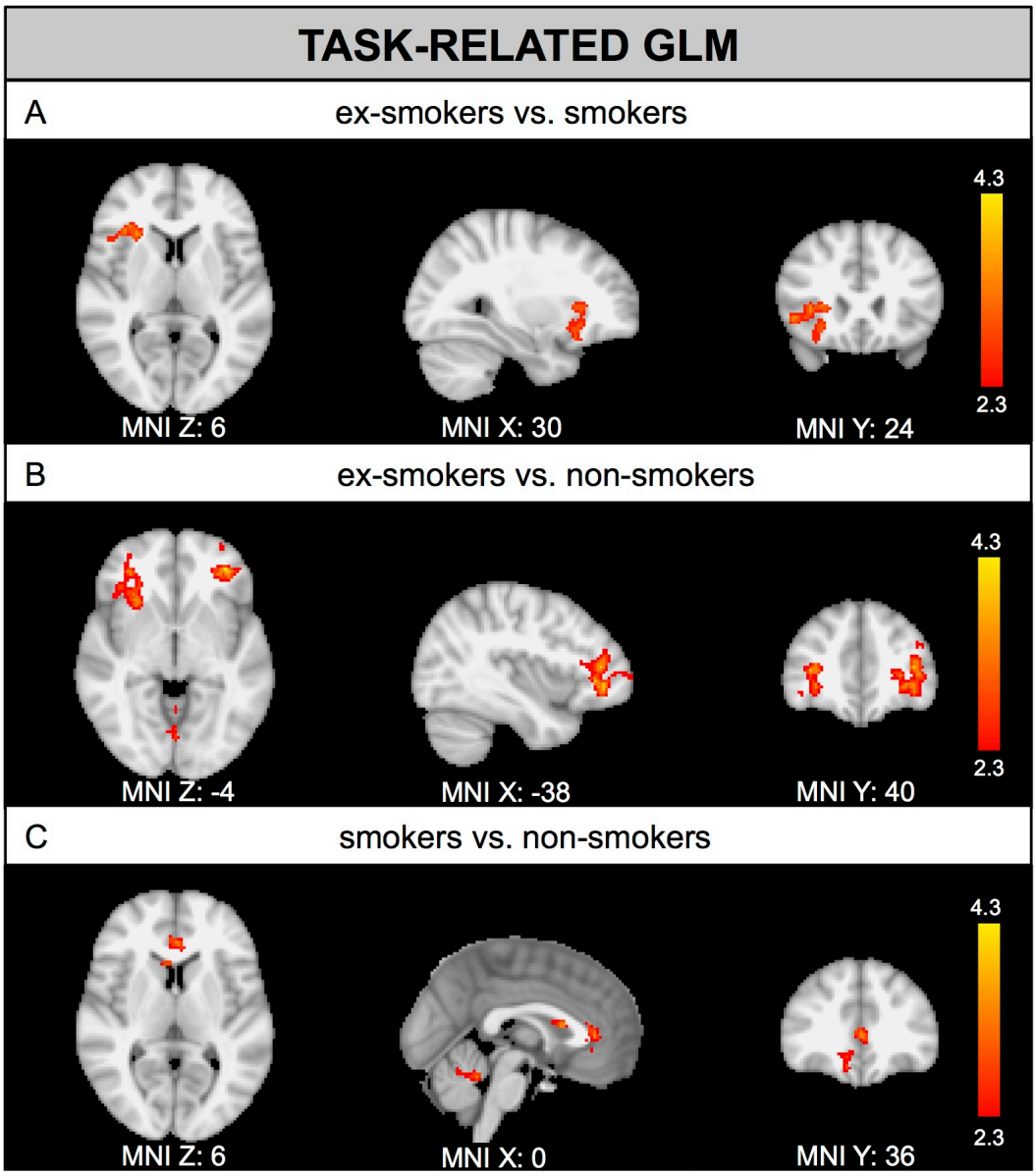

Figure 3: TASK-RELATED GLM ANALYSES FOR THE COMPARISON OF SMOKING VIDEOS VS CONTROL VIDEOS.
Ex-smokers versus smokers (Figure 3A) had increased activations notably in the right anterior insula, frontal operculum and inferior frontal gyrus.
Ex-smokers versus non-smokers (Figure 3B) had increased activations notably in the bilateral frontal pole inferior frontal gyrus and right anterior insula. Smokers versus non-smokers (Figure 3C) had higher activations notably in the ventral anterior cingulate cortex. The inverse comparisons of smokers versus ex-smokers, non-smokers versus ex-smokers and non-smokers versus smokers yielded no supra-threshold activations. Activations are superimposed on the template brain in MNI space, cluster threshold at Z=2.3 corresponding to p=0.05 (corrected).

3.3. Correlation Between Imaging Data and Accumulated Cigarettes Consumption

A positive correlation was found between the cumulative cigarette dose (pack-years) and the time course extracted from the COPE images for the contrast smoking videos versus control videos in the Single Subject Task-related GLM (P<.05) (Figure4). No correlations were found for other behavioral measures.

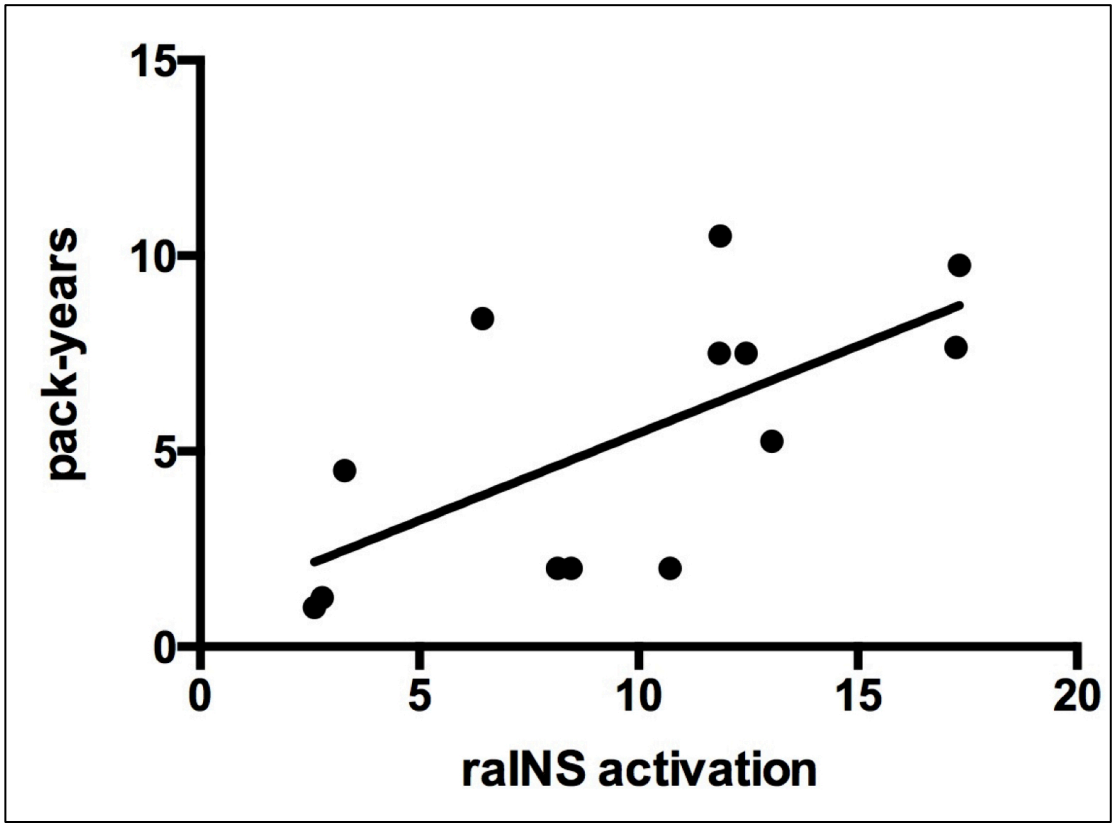

Figure 4: CORRELATION BETWEEN NICOTINE DOSE AND FMRI ACTIVATION IN RIGHT ANTERIOR INSULA IN EX-SMOKERS
Correlation in ex-smokers between the accumulated nicotine dose (measured in pack-years) and the fMRI activation strength in the right anterior insula measured as contrast of parameter estimates (COPE) for the contrast of smoking cue videos versus control videos, which was significant at $p < 0.05$.

3.4. Seed based Functional Connectivity

The one-sample t-tests showed a significant effect of connectivity for all connections (p<.0001). Only the ANOVA performed on the connection raINS-ACC showed a significant group difference (p<.01). For this connection, post-hoc tests revealed statistical differences between non-smokers and smokers (p<.01), and between non-smokers and ex-smokers (p<.05). No significant differences were found for the comparison between smokers and ex-smokers (Figure 5).

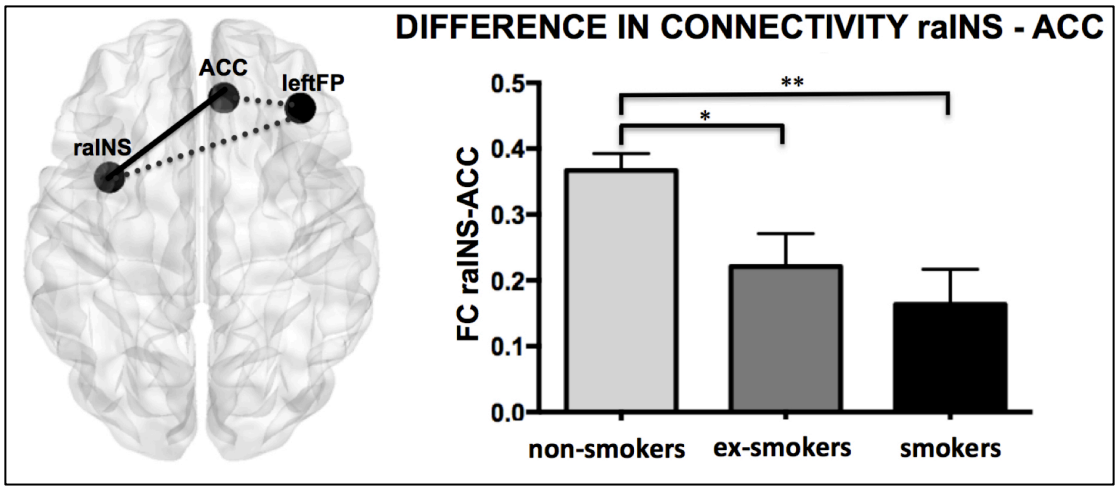

Figure 5: FUNCTIONAL CONNECTIVITY BETWEEN THE THREE KEY REGIONS
All three regions (raINS, ACC and leftFP) were significantly connected in all three groups. The comparison between ex-smokers versus active smokers and controls revealed that ex-smokers (p<0.05) and active smokers (p<0.01) had significantly reduced connectivity between raINS and ACC, while there was no significant difference between ex-smokers and active smokers. The barplots indicate mean values with SE. * p<0.05, ** p<0.01.

3.5. VBM and TBSS Analysis

The VBM analysis of the Gray Matter (GM) and the TBSS analysis of the White Matter (WM) revealed no statistical differences between the groups.

4. DISCUSSION

The current investigation aims to understand the neural mechanisms that promote long-term nicotine abstinence, looking at ex-smokers. Our results show that the right anterior insula (raINS) plays a main role in long-term craving regulation, controlling the activation of areas related to craving urge as the ventral anterior cingulate cortex (vACC). The strength of the raINS activity is associated to the pack-years (nicotine dose). Finally, a persistent disruption in connectivity in the group smokers compared to non-smokers can be identified, with ex-smokers that occupy an intermediate position.

In this study, the results of the Task-related GLM for the contrast smoking videos vs. control videos confirm previous findings, showing the involvement of brain regions related to craving urge in smokers compared to non-smokers, through the activation of the ventral anterior cingulate cortex (Brody et al., 2004; Azizian et al., 2010; Brody et al., 2007; Wang et al., 2007). For the same contrast, the ex-smokers compared to non-smokers show a persistent higher activation of bilateral frontal areas as the anterior insula and the pre-frontal cortex. The key role of the anterior insula is confirmed also in the contrast ex-smokers vs. smokers, where this region is significantly more active for the group ex-smokers. These results are consistent with the ones from previous studies on smokers and on short-term nicotine abstinence, identifying frontal regions as responsible of craving regulation and inhibition (Nestor et al.,2011; Blasi et al., 2006; Wang et al., 2007; Kober et al., 2010;Wilson et al., 2005).

The importance of the insula in craving and drug seeking is shown in particular in a review by Naqvi (Naqvi *et al*, 2014) demonstrating its three different and even opposite functions of incentive motivational processes that can drive addictive behavior, control processes that can inhibit and moderate addictive behavior and interoceptive processes that represent bodily states associated with drug use. The current investigation extends previous studies on short-term nicotine abstinence, identifying the raINS as the key region responsible of regulation during the whole withdrawal period through the enhancement and the inhibition of areas related to cigarettes craving also in long-term cigarette abstinence. In particular, in our study this enhancement of inhibition decreases vACC activity.

Furthermore, the activity in the raINS in ex-smokers correlates with the nicotine dose (pack-years). Following the previous interpretation, we can conclude that the higher the number of smoked cigarettes and longer the period of smoking, the stronger is the raINS activation necessary to inhibit the ACC.

To analyze the connectivity between these regions, the seed based functional connectivity analysis was performed choosing as seed regions the raINS and the ACC. This choice was based on the task-related GLM results and on previous literature found on this topic (Nestor, McCabe, Jones, Clancy, & Garavan, 2011). Looking at the ANOVA results, the connectivity between the two regions is significantly higher in non-smokers compared to smokers, while the ex-smokers occupy an intermediate position between the two other

groups. Due to these results, we can come to the conclusion that the functional connectivity between these areas decreases for subjects under smoking addiction and this leads to a failure in regulating areas related to the craving system. These connectivity results are coherent with a recent study showing decreased connectivity in active smokers versus non-smokers between dorsolateral prefrontal cortex and parietal nodes that are part of the executive control network (ECN) (Weiland *et al*, 2014). Our results are also in line with findings from studies on several other forms of addiction, from opioids (Liu et al., 2009; Ma et al., 2011; Upadhyay et al., 2010) to internet addiction (Hong et al., 2013) where a lower functional connectivity is present in addicted subjects. Our results are, however, in conflict with previous findings that demonstrated an increase in connectivity between prefrontal areas in active smokers (Janes *et al*, 2012). This difference can be due to the fact that the functional connectivity was identified through a data-driven approach of resting-state fMRI paradigm, while we have studied task-based connectivity driven by the processing of video cues that directly induced craving urge. Most importantly, these other studies assessed active smokers, and no previous study to date has investigated brain connectivity during long-term nicotine abstinence in ex-smokers.

Nevertheless, it's important to notice that some limitations are present in this study and that they can influence the interpretation of the results. First, the number of the participants in each group is small and we did not employ a structured clinical interview for DSM-IV Axis I diagnoses during the participants recruitment to form the different groups. In addition, even if the

smokers could smoke ad libidum prior to testing, withdrawal from and cravings for nicotine may have had an effect on the task, and consequently, on our results. Furthermore, the functional connectivity in our study is conditioned by the presentation of smoking videos stimulations, so the results reflect a connectivity driven by the research paradigm and they are hardly comparable to the results of other studies that used resting-state connectivity measures. Finally, it's important to underline that possible confounding results from structural changes in White or Gray Matter can be present. To avoid this, VBM and TBSS analyses were conducted and no differences were observed between the three groups.

5. CONCLUSION

The aim of this study was to investigate, through the presentation of smoking related videotapes, which brain areas are responsible of craving regulation during long-term nicotine abstinence (ex-smoker subjects), which behavioral components are related to the activations in the found areas and how the functional connectivity changes into the three groups. Our results suggest mechanisms underlying the promotion of the long-term nicotine abstinence, studying ex-smokers. The findings of this work can be useful for futures investigations and interventions to support patients quitting tobacco addiction.

6. REFERENCES

Azizian A, Nestor LJ, Payer D, Monterosso JR, Brody AL, London ED (2010). Smoking reduces conflict-related anterior cingulate activity in abstinent cigarette smokers performing a Stroop task. *Neuropsychopharmacology* **35**: 775–782.

Brady, J.M. S S. (1997). SUSAN - a new approach to low level image processing. *International Journal of Computer Vision* .

Brody AL, Mandelkern MA, Lee G, Smith E, Sadeghi M, Saxena S, *et al* (2004). Attenuation of cue-induced cigarette craving and anterior cingulate cortex activation in bupropion-treated smokers: a preliminary study. *Psychiatry Res* **130**: 269–281.

Brody AL, Mandelkern MA, Olmstead RE, Jou J, Tiongson E, Allen V, *et al* (2007). Neural substrates of resisting craving during cigarette cue exposure. *Biol Psychiatry* **62**: 642–651.

Carroll AJ, Sutherland MT, Salmeron BJ, Ross TJ, Stein EA (2013). Greater externalizing personality traits predict less error-related insula and anterior cingulate cortex activity in acutely abstinent cigarette smokers. *Addict Biol* doi:10.1111/adb.12118.

Culbertson CS, Bramen J, Cohen MS, London ED, Olmstead RE, Gan JJ, *et al* (2011). Effect of bupropion treatment on brain activation induced by cigarette-related cues in smokers. *Arch Gen Psychiatry* **68**: 505–515.

DeBry SC, Tiffany ST (2008). Tobacco-induced neurotoxicity of adolescent cognitive development (TINACD): a proposed model for the development of impulsivity in nicotine dependence. *Nicotine Tob Res* **10**: 11–25.

Devlin H, Tracey I, Johansen-Berg H, Stuart C (2005). What is Functional Magnetic Resonance Imaging (fMRI)? .

Ding X, Lee S-W (2013). Changes of functional and effective connectivity in smoking replenishment on deprived heavy smokers: a resting-state FMRI study. *PLoS ONE* **8**: e59331.

Fritz H-C, Wittfeld K, Schmidt CO, Domin M, Grabe HJ, Hegenscheid K, *et al* (2014). Current smoking and reduced gray matter volume-a voxel-based morphometry study. *Neuropsychopharmacology* **39**: 2594–2600.

Garavan H, Pankiewicz J, Bloom A, Cho JK, Sperry L, Ross TJ, *et al* (2000). Cue-induced cocaine craving: neuroanatomical specificity for drug users and drug stimuli. *Am J Psychiatry* **157**: 1789–1798.

Gardner EL (2011). Addiction and brain reward and antireward pathways. *Adv Psychosom Med* **30**: 22–60.

Geier CF, Sweitzer MM, Denlinger R, Sparacino G, Donny EC (2014). Abstinent adult daily smokers show reduced anticipatory but elevated saccade-related brain responses during a rewarded antisaccade task. *Psychiatry Res* **223**: 140–147.

George O, Koob GF (2013). Control of craving by the prefrontal cortex. *Proc Natl Acad Sci USA* **110**: 4165–4166.

Gualano MR, Passi S, Bert F, Torre G La, Scaioli G, Siliquini R (2014). Electronic cigarettes: assessing the efficacy and the adverse effects through a systematic review of published studies. *J Public Health (Oxf)* doi:10.1093/pubmed/fdu055.

Hendricks PS, Prochaska JJ, Humfleet GL, Hall SM (2008). Evaluating the validities of different DSM-IV-based conceptual constructs of tobacco dependence. *Addiction* **103**: 1215–1223.

Holmes S, Zwar N, Jiménez-Ruiz CA, Ryan PJ, Browning D, Bergmann L, *et al* (2004). Bupropion as an aid to smoking cessation: a review of real-life effectiveness. *Int J Clin Pract* **58**: 285–291.

Hong S-B, Zalesky A, Cocchi L, Fornito A, Choi E-J, Kim H-H, *et al* (2013). Decreased functional brain connectivity in adolescents with internet addiction. *PLoS ONE* **8**: e57831.

Hughes JR, Lesmes GR, Hatsukami DK, Richmond RL, Lichtenstein E, Jorenby DE, *et al* (1999). Are higher doses of nicotine replacement more effective for smoking cessation? *Nicotine Tob Res* **1**: 169–174.

Hurt RD, Sachs DP, Glover ED, Offord KP, Johnston JA, Dale LC, *et al* (1997). A comparison of sustained-release bupropion and placebo for smoking cessation. *N Engl J Med* **337**: 1195–1202.

Janes AC, Nickerson LD, Frederick BDB, Kaufman MJ (2012). Prefrontal and limbic resting state brain network functional connectivity differs between nicotine-dependent smokers and non-smoking controls. *Drug Alcohol Depend* **125**: 252–259.

Jenkinson M, Bannister P, Brady M, Smith S (2002). Improved optimization for the robust and accurate linear registration and motion correction of brain images. *Neuroimage* **17**: 825–841.

Jorenby DE, Leischow SJ, Nides MA, Rennard SI, Johnston JA, Hughes AR, *et al* (1999). A controlled trial of sustained-release bupropion, a nicotine patch, or both for smoking cessation. *N Engl J Med* **340**: 685–691.

Jougasaki M, Yasue H, Takahashi K (1989). Perivascular nerve lesion of the coronary artery involved in spasm in a patient with variant angina. *Pathology* **21**: 304–307.

Killen JD, Fortmann SP, Davis L, Strausberg L, Varady A (1999). Do heavy smokers benefit from higher dose nicotine patch therapy? *Exp Clin Psychopharmacol* **7**: 226–233.

Killen JD, Fortmann SP, Schatzberg AF, Hayward C, Sussman L, Rothman M, *et al* (2000). Nicotine patch and paroxetine for smoking cessation. *J Consult Clin Psychol* **68**: 883–889.

Kober H, Mende-Siedlecki P, Kross EF, Weber J, Mischel W, Hart CL, *et al* (2010). Prefrontal-striatal pathway underlies cognitive regulation of craving. *Proc Natl Acad Sci USA* **107**: 14811–14816.

Koob GF, Volkow ND (2010). Neurocircuitry of addiction. *Neuropsychopharmacology* **35**: 217–238.

Lee E, Ku J, Jung Y-C, Lee H, An SK, Kim KR, *et al* (2013). Neural evidence for emotional involvement in pathological alcohol craving. *Alcohol Alcohol* **48**: 288–294.

Lerman C, Gu H, Loughead J, Ruparel K, Yang Y, Stein EA (2014). Large-scale brain network coupling predicts acute nicotine abstinence effects on craving and cognitive function. *JAMA Psychiatry* **71**: 523–530.

Liu J, Liang J, Qin W, Tian J, Yuan K, Bai L, *et al* (2009). Dysfunctional connectivity patterns in chronic heroin users: an fMRI study. *Neurosci Lett* **460**: 72–77.

Luigjes J, Brink W van den, Feenstra M, Munckhof P van den, Schuurman PR, Schippers R, *et al* (2012). Deep brain stimulation in addiction: a review of potential brain targets. *Mol Psychiatry* **17**: 572–583.

Ma N, Liu Y, Fu X-M, Li N, Wang C-X, Zhang H, *et al* (2011). Abnormal brain default-mode network functional connectivity in drug addicts. *PLoS ONE* **6**: e16560.

Monti MM (2011). Statistical Analysis of fMRI Time-Series: A Critical Review of the GLM Approach. *Front Hum Neurosci* **5**: 28.

Morales AM, Ghahremani D, Kohno M, Hellemann GS, London ED (2014). Cigarette exposure, dependence, and craving are related to insula thickness in young adult smokers. *Neuropsychopharmacology* **39**: 1816–1822.

Naqvi NH, Gaznick N, Tranel D, Bechara A (2014). The insula: a critical neural substrate for craving and drug seeking under conflict and risk. *Ann N Y Acad Sci* **1316**: 53–70.

Naqvi NH, Rudrauf D, Damasio H, Bechara A (2007). Damage to the insula disrupts addiction to cigarette smoking. *Science* **315**: 531–534.

Nestor L, McCabe E, Jones J, Clancy L, Garavan H (2011). Differences in “bottom-up” and “top-down” neural activity in current and former cigarette smokers: Evidence for neural substrates which may promote nicotine abstinence through increased cognitive control. *Neuroimage* **56**: 2258–2275.

Polosa R, Caponnetto P, Morjaria JB, Papale G, Campagna D, Russo C (2011). Effect of an electronic nicotine delivery device (e-Cigarette) on smoking reduction and cessation: a prospective 6-month pilot study. *BMC Public Health* **11**: 786.

Smith SM (2002). Fast robust automated brain extraction. *Hum Brain Mapp* **17**: 143–155.

Smith SM, Jenkinson M, Johansen-Berg H, Rueckert D, Nichols TE, Mackay CE, *et al* (2006). Tract-based spatial statistics: voxelwise analysis of multi-subject diffusion data. *Neuroimage* **31**: 1487–1505.

Smith SM, Jenkinson M, Woolrich MW, Beckmann CF, Behrens TEJ, Johansen-Berg H, *et al* (2004). Advances in functional and structural MR image analysis and implementation as FSL. *Neuroimage* **23 Suppl 1**: S208–219.

Smith SM, Johansen-Berg H, Jenkinson M, Rueckert D, Nichols TE, Miller KL, *et al* (2007a). Acquisition and voxelwise analysis of multi-subject diffusion data with tract-based spatial statistics. *Nat Protoc* **2**: 499–503.

Smith SM, Johansen-Berg H, Jenkinson M, Rueckert D, Nichols TE, Miller KL, *et al* (2007b). Acquisition and voxelwise analysis of multi-subject diffusion data with tract-based spatial statistics. *Nat Protoc* **2**: 499–503.

Sweitzer MM, Geier CF, Joel DL, McGurrin P, Denlinger RL, Forbes EE, *et al* (2013). Dissociated Effects of Anticipating Smoking versus Monetary Reward in the Caudate as a Function of Smoking Abstinence. *Biol Psychiatry* **76**: 681–688.

Upadhyay J, Maleki N, Potter J, Elman I, Rudrauf D, Knudsen J, *et al* (2010). Alterations in brain structure and functional connectivity in prescription opioid-dependent patients. *Brain* **133**: 2098–2114.

Wang Z, Faith M, Patterson F, Tang K, Kerrin K, Wileyto EP, *et al* (2007). Neural substrates of abstinence-induced cigarette cravings in chronic smokers. *J Neurosci* **27**: 14035–14040.

Weiland BJ, Sabbineni A, Calhoun VD, Welsh RC, Hutchison KE (2014). Reduced executive and default network functional connectivity in cigarette smokers. *Hum Brain Mapp* doi:10.1002/hbm.22672.

Whitwell JL (2009). Voxel-based morphometry: an automated technique for assessing structural changes in the brain. *J Neurosci* **29**: 9661–9664.

Wilson SJ, Sayette MA, Delgado MR, Fiez JA (2005). Instructed smoking expectancy modulates cue-elicited neural activity: a preliminary study. *Nicotine Tob Res* **7**: 637–645.

Winkler AM, Ridgway GR, Webster MA, Smith SM, Nichols TE (2014). Permutation inference for the general linear model. *Neuroimage* **92**: 381–397.

Yu R, Zhao L, Lu L (2011). Regional grey and white matter changes in heavy male smokers. *PLoS ONE* **6**: e27440.

(2014). Clearing the smoke. *Nat Neurosci* **17**: 1013.

European Union Campaign, 2013, n.d. Ex-smokers are Unstoppable.

OECD (2012a), OECD Health Data 2012, Online, OECD Publishing, Paris, available at: www.oecd.org/health/ healthdata.

7. APPENDIX

7.1. Supplementary figures

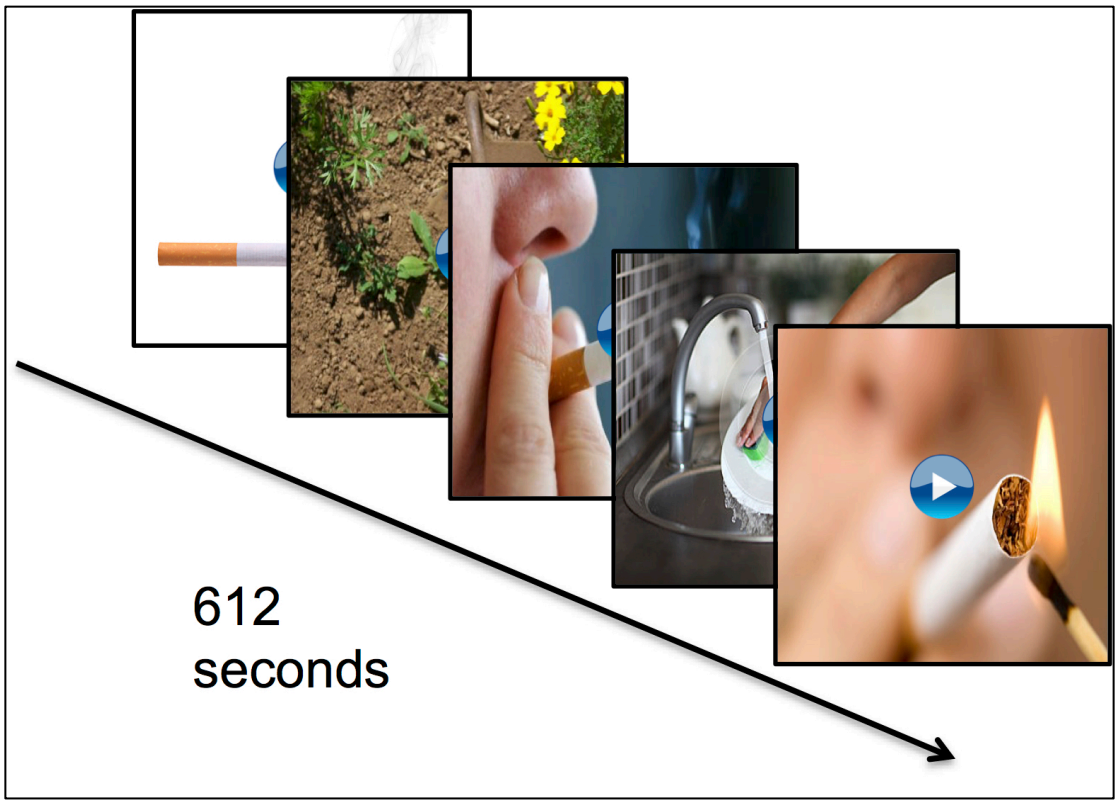

Supplementary figure A. The paradigm consisted of an on-off block-design with two active conditions (smoking cue and control videos) and a rest condition. The active condition used video cues developed by Brody (Brody *et al*, 2007; Culbertson *et al*, 2011). These cues were filmed from the first person point of view and were 45 sec in length. Each smoking video shows a potential craving situation, such as writing a letter and smoking a cigarette or standing outside of a nightclub smoking a cigarette. The control videos were matched for similar content except for the absence of smoking cues. After each video, a visual analog scale was presented for 2.5 seconds and participants rated the degree of craving using an MR-compatible response box. The rating scale included seven steps from no craving to high craving. After the rating, a rest period consisted of the visual presentation of a fixation cross for 10 seconds. Each run included 5 smoking and 5 control videos in a pseudo-randomized fashion and lasted 612 seconds (Supplementary Figure A).

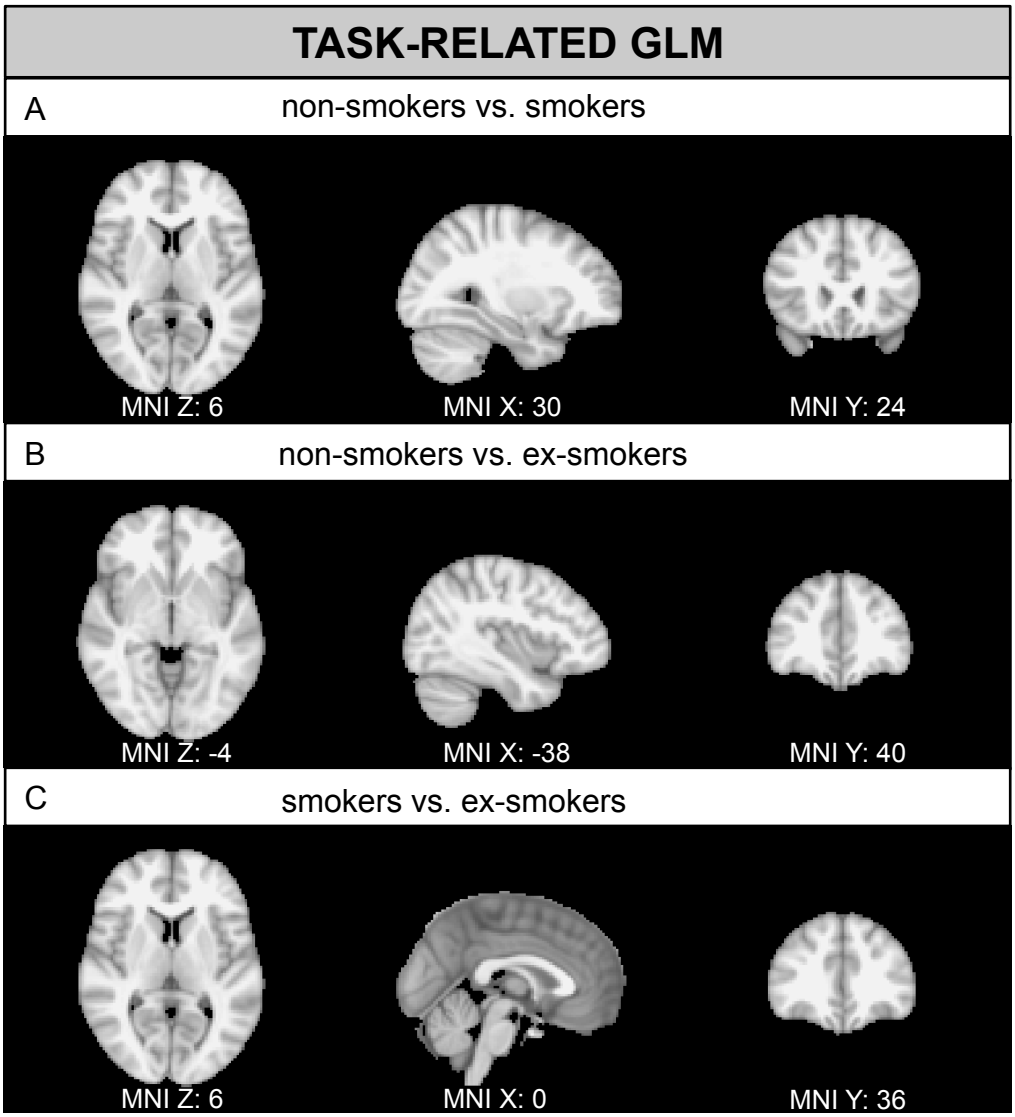

Supplementary figure B. illustrates the opposite comparisons with respect to figure 2. There were no supra-threshold activations for ex-smokers versus smokers (A), ex-smokers versus non-smokers (B) or smokers versus non-smokers (C).

7.2. Supplementary tables

TableA Task-Related GLM

Smokers vs. non-smokers

Cluster Index	Voxels	P	-log10(P)	Z-MAX	Position	Z-MAX X (mm)	Z-MAX Y (mm)	Z-MAX Z (mm)	Z-COG X (mm)	Z-COG Y (mm)	Z-COG Z (mm)	COPE-MAX	COPE-MAX X (mm)	COPE-MAX Y (mm)	COPE-MAX Z (mm)	COPE-MEAN		Regions
1	544	0.00575	2.24	3.6	-8,-56,-16	-8	-56	-16	-1.58	-47.8	-23.2	19.4	-16	-30	-26	8.94	B	Cerebellum
2	494	0.0105	1.98	3.72	2,14,14	2	14	14	5.43	26	5.28	17.4	0	36	6	8.89	B	Anterior Cingulate Cortex Right Lateral Ventricle

Ex-smokers vs. non-smokers

Cluster Index	Voxels	P	-log10(P)	Z-MAX	Position	Z-MAX X (mm)	Z-MAX Y (mm)	Z-MAX Z (mm)	Z-COG X (mm)	Z-COG Y (mm)	Z-COG Z (mm)	COPE-MAX	COPE-MAX X (mm)	COPE-MAX Y (mm)	COPE-MAX Z (mm)	COPE-MEAN		Regions
1	2177	2.12E-09	8.67	3.9	2,-52,-26	2	-52	-26	-3.13	-49	-21.6	19.1	-14	-28	-18	9.47	B	Cerebellum
2	1078	0.00000207	4.68	4.12	36,44,-2	-36	44	-2	-35.1	43.8	7.4	35.8	-30	64	4	10.5	L	Frontal Pole Inferior Frontal Gyrus Anterior Insula
3	954	0.000069	4.16	4.04	38,44,8	38	44	8	33.8	34.3	-2.28	16.1	24	58	-12	8.31	R	Anterior Insula Frontal Pole Inferior Frontal Gyrus

Ex-smokers vs. smokers

Cluster Index	Voxels	P	-log10(P)	Z-MAX	Position	Z-MAX X (mm)	Z-MAX Y (mm)	Z-MAX Z (mm)	Z-COG X (mm)	Z-COG Y (mm)	Z-COG Z (mm)	COPE-MAX	COPE-MAX X (mm)	COPE-MAX Y (mm)	COPE-MAX Z (mm)	COPE-MEAN		Regions
1	391	0.0388	1.41	3.42	28,2 2,6	28	22	6	36.2	23.7	-2.46	21.4	50	20	-8	10.2	R	Anterior Insula Frontal Operculum Inferior Frontal Gyrus